Annals of Biomedical Engineering, Vol. 33, No. 8, August 2005 (© 2005) pp. 1015–1026
DOI: 10.1007/s10439-005-5758-z

A Computer Reconstruction of the Entire Coronary Arterial Tree Based on Detailed Morphometric Data

N. MITTAL,[1] Y. ZHOU,[2] S. UNG,[1] C. LINARES,[1] S. MOLLOI,[3] and G. S. KASSAB[1]

[1]Department of Biomedical Engineering, University of California, Irvine, CA; [2]Cedars-Sinai Medical Center, Los Angeles, CA; [3]Department of Radiological Sciences, University of California, Irvine, CA

(Received 7 April 2004; accepted 28 March 2005)

Abstract—A rigorous analysis of blood flow must be based on the branching pattern and vascular geometry of the full vascular circuit of interest. It is experimentally difficult to reconstruct the entire vascular circuit of any organ because of the enormity of the vessels. The objective of the present study was to develop a novel method for the reconstruction of the full coronary vascular tree from partial measurements. Our method includes the use of data on those parts of the tree that are measured to extrapolate the data on those parts that are missing. Specifically, a two-step approach was employed in the reconstruction of the entire coronary arterial tree down to the capillary level. Vessels >40 μm were reconstructed from cast data while vessels <40 μm were reconstructed from histological data. The cast data were reconstructed one-bifurcation at a time while histological data were reconstructed one-sub-tree at a time by "cutting" and "pasting" of data from measured to missing vessels. The reconstruction algorithm yielded a full arterial tree down to the first capillary bifurcation with 1.9, 2.04 and 1.15 million vessel segments for the right coronary artery (RCA), left anterior descending (LAD) and left circumflex (LCx) trees, respectively. The node-to-node connectivity along with the diameter and length of every vessel segment was determined. Once the full tree was reconstructed, we automated the assignment of order numbers, according to the diameter-defined Strahler system, to every vessel segment in the tree. Consequently, the diameters, lengths, number of vessels, segments-per-element ratio, connectivity and longitudinal matrices were determined for every order number. The present model establishes a morphological foundation for future analysis of blood flow in the coronary circulation.

Keywords—Strahler system, Diameter-Defined Strahler system, Vascular reconstruction, Growth algorithm, Design rules.

INTRODUCTION

Any realistic hemodynamic analysis of blood flow must be based on a complete vascular circuit of the organ of interest. The morphometric data on the branching pattern (connectivity of one branch to another) and geometry (diameters and lengths) of the vascular circuit must be known. An inherent difficulty, however, is that the vascular tree has too many branches to be counted like a census of a nation's population. Furthermore, it is impossible to experimentally obtain a complete cast of the entire vascular tree down to the capillary vessels because even a tiny air bubble in the cast material may prevent the filling of some parts of the coronary tree or because the fragile small branches of the cast are easily broken. Hence, it is important to develop a method for extrapolating a full vascular tree from an incomplete cast or image.

The objective of the present study is to develop a computer algorithm to generate a full vascular coronary tree from a partially measured tree. Our approach is to use the data on those parts of the tree that are measured to extrapolate the data on those parts that are missing. In the process, the proximal branches obtained from cast measurements (including the epicardial and larger penetrating vessels) are completely known while the micro-vessels are statistically reconstructed from the histological data. The premise of this approach is that the larger vessels are few in numbers and should be known exactly while the smaller vessels are much larger in numbers and can be known statistically.

Kassab and colleagues have previously measured the morphometric data of the anatomy of the pig coronary arteries,[11,13] capillaries[10] and veins.[12] In the process, they added four new innovations to morphometry:[8,11] the Diameter-Defined Strahler ordering system for assigning the order numbers of the vessels, the distinction between series and parallel vessel segments, the connectivity matrix to describe the asymmetric branching pattern of vessels, and the longitudinal position matrix to describe the longitudinal position of daughter vessels along the length of their parent vessels. This endevaor was accomplished manually and hence the program took several years to accomplish. The goal of the present study was to develop a computer algorithm to extract a full tree from partial measurements and to automate the diameter-defined Strahler system to obtain detailed morphometric data on the diameters, lengths, number of vessels, connectivity and longitudinal position matrices from the full reconstructed tree. This is the first

Address correspondence to Ghassan S. Kassab, Ph.D., Department of Biomedical Engineering, University of California, Irvine, 204 Rockwell Engineering Center, Irvine, CA 92697-2715. Electronic mail: gkassab@uci.edu

step towards automation of vascular reconstruction and will markedly accelerate the data analysis process. It will also provide a definitive tree with full connectivity (node-to-node connectivity) and geometry (segment diameter and length) which is amenable to hemodynamic simulations. The automation of data measurements remains a laudable goal for future studies.

METHODS

Available Data

Previously, Kassab *et al.*[11] have described in detail the methods of preparation, measurement and morphometric analysis of the entire coronary arterial tree. Briefly, the morphometric data on the coronary arterial vessels of diameters <40 μm were obtained from histological specimens. Plugs of myocardial tissue were removed from the left ventricles (LV) and right ventricles (RV) of cast hearts. Each plug was completely sectioned transmurally into 60- to 80-μm thickness. Each section was dehydrated with 100% alcohol and cleared with methyl salicylate to render the myocardium transparent and the elastomer-filled microvasculature visible under a light microscope. The morphometry of the coronary arterioles and venules was reconstructed through optical sectioning as described previously.[11]

The morphometric data on the coronary arterial vessels of diameters >40 μm were obtained from cast studies. The right coronary artery (RCA), left anterior descending (LAD) and left circumflex (LCx) arterial casts were dissected and viewed with a stereo-dissection microscope and displayed on a video monitor through a television camera as described in Kassab *et al.*[11] The images were grabbed by a digitizing system and analyzed using computer software. Several lumen diameter measurements were made along each vessel segment to obtain a mean diameter, and the vessel segmental length were obtained by measuring the distance between bifurcation points along the centerline of the vessel. The trunks of the coronary arteries were sketched and their segments measured. The subtrees arising from the trunk were labeled, excised, placed in separate jars, further sketched and measured. This process was continued until the entire RCA, LAD and LCx arterial tree casts were sketched and their morphometric measurements made. Since it is not possible to obtain a complete cast of the arterial tree down to the capillary vessels, the vessels are invariably "broken" or "missing" at some dimension greater than the capillaries (≥ 8 μm). The diameter distributions of broken or terminal vessels of the cast data are shown in Fig. 1 with mean $\pm$ SD of 61.1 ± 42.4, 75.9 ± 52.6 and 97.9 ± 55.3 μm for the RCA, LAD and LCx, respectively. The distributions are seen to be skewed with medians of 50.2 (RCA), 63.3 (LAD) and 84.7 μm (LCx).

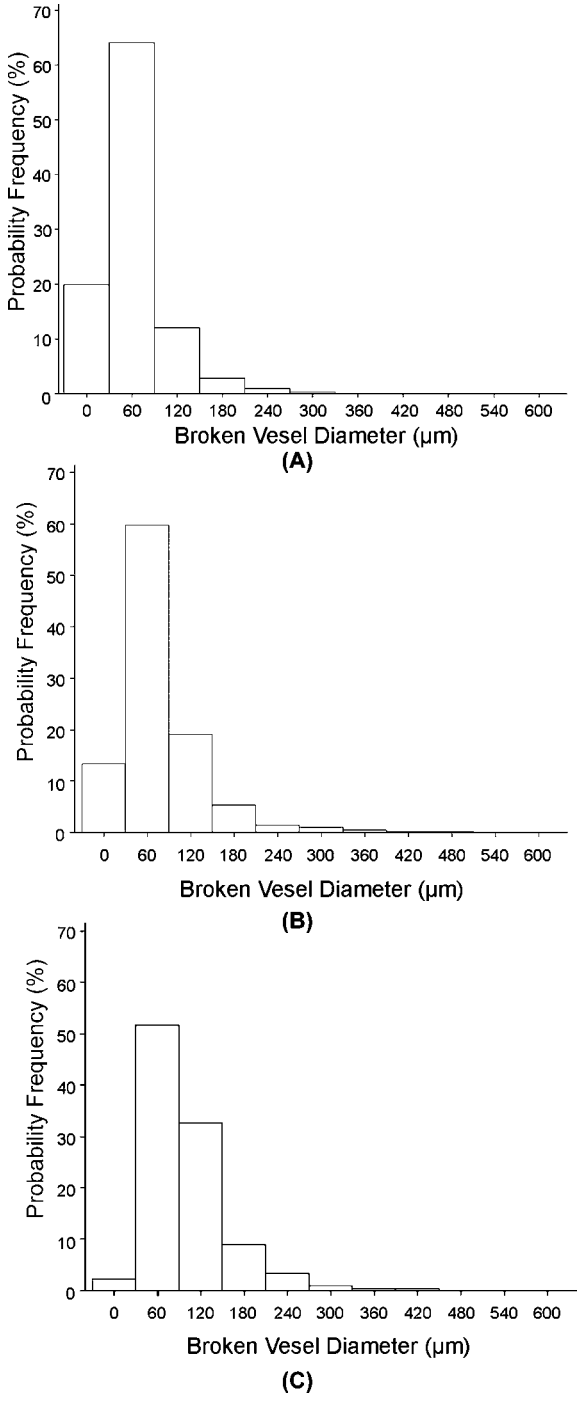

FIGURE 1. The probability frequency distribution for the diameter of broken vessels in the cast of (A) RCA, (B) LAD and (C) LCx tree.

Reconstruction Algorithm

A two-step approach was employed in the reconstruction of the entire coronary arterial tree down to the capillary level (≤ 8 μm in diameter). Portions of the arterial tree (RCA, LAD or LCx artery) missing from the cast data were

computationally reconstructed from anatomical data. Missing components of the tree, from broken vessel segments down to vessels of diameter 40 μm, were reconstructed from the intact cast data. Portions of the tree made up of vessels with diameter <40 μm were reconstructed based on histological data. Reconstructed networks were terminated at segments of diameter $\leq$8 μm. Any terminal vessels in the cast data with diameter >8 μm was treated as a broken vessel and the reconstruction algorithm was applied to generate a sub-tree that branched down to the arterial capillaries of diameter $\leq$8 μm.

Input Files

Initially, the node-to-node connections of the entire cast data of each arterial tree (RCA, LAD or LCx) were stored as input files while the hundreds of non-contiguous arteriolar micro-vessels (LV or RV) were stored in separate files. In addition to the node-to-node connectivity, the input files also contained diameter and length data of each vessel segment (with the exception of cut vessels which only had diameters). Hence, the branching pattern and vascular geometry of all the previously reconstructed data on hard records[11] were transformed into digital Excel files. The data files are made available to the public via the website http://cvbiomech.eng.uci.edu.

A computer program adapted from CISpace: Tools for Learning Computational Intelligence (http://www.cs.ubc.ca/labs/lci/CIspace/index.html)[17] was used to enter the node-to-node connections graphically. This Graphical Tool Kit can generate tab-delimited text files from any tree of interest for the single cast tree and the numerous arteriolar trees. An example of this graphical representation is shown in Fig. 2 for an arteriolar tree. The corresponding tabular format for the example tree is shown in Table 1. The first and second columns in the table each uniquely identify a particular vessel and specify the mother-daughter connection. The first column refers to the vessel itself, whereas the second column refers to the mother vessel. The third column contains the position of the vessel branch relative to the mother ('*R*' for right and '*L*' for left) and the last two columns contain the diameter and length of the vessel in micrometers. A "−2" in the length column signifies a broken vessel whose length is unknown.

Cast Data

The growth of a broken or terminal cast vessel >40 μm entailed the search of intact bifurcations (for which mother and the two daughter vessel were measured) with mother diameter closest (smallest difference) to the terminal vessel. Once such a bifurcation was found, it was "pasted" to the broken vessel. A search was then made for each of the two

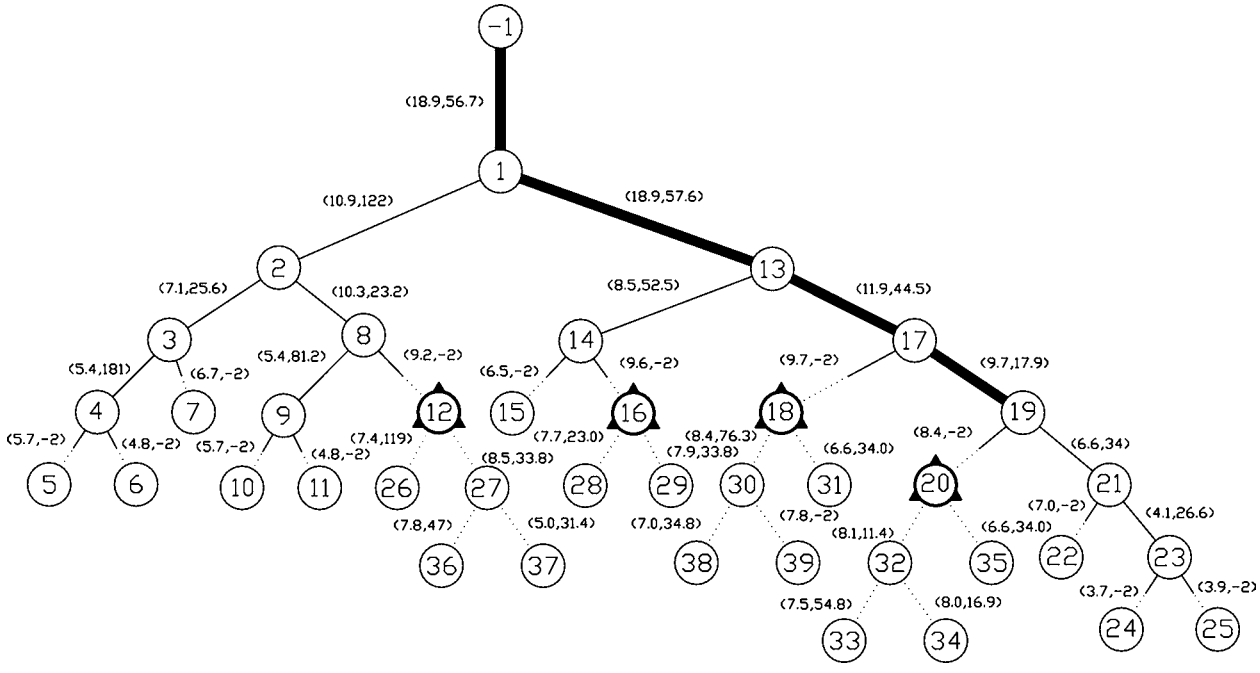

FIGURE 2. A schematic of an arteriolar tree with the nodes labeled numerically and the segment diameters and lengths specified. The first and second numbers in the parentheses correspond to the diameter and length of the segment, respectively. The "−2" denotes a broken vessel whose length is unknown. The heavy line corresponds to the trunk of the arteriole tree. The partly "solid" and partly "dashed" segments correspond to broken vessels >8 μm which were "grown" using the proposed algorithm. The entirely "dashed" segments correspond to "grown" vessels.

TABLE 1. Sample input file for the arteriolar tree shown in Figure 1.

Node label	Mother label	Direction	Diameter (μm)	Length (μm)
1	−1	ROOT	18.9	56.7
2	1	L	10.9	122
3	2	L	7.1	25.6
4	3	L	5.4	181
5	4	L	5.7	−2
6	4	R	4.8	−2
7	3	R	6.7	−2
8	2	R	10.3	23.2
9	8	L	5.4	81.2
10	9	L	5.7	−2
11	9	R	4.8	−2
12	8	R	9.2	−2
13	1	R	18.9	57.6
14	13	L	8.5	52.5
15	14	L	6.5	−2
16	14	R	9.6	−2
17	13	R	11.9	44.5
18	17	L	9.7	−2
19	17	R	9.7	17.9
20	19	L	8.4	−2
21	19	R	6.6	34
22	21	L	7	−2
23	21	R	4.1	26.6
24	23	L	3.7	−2
25	23	R	3.9	−2

daughter vessels of the "pasted" bifurcation and so on. This process was repeated until the tree was reconstructed down to approximately 40 μm. The search was made more efficient by arranging the intact input diameters into bins. This significantly reduced the search of data to find the closest match. Since the data entry associates the mother vessel with its larger and smaller daughter vessels, the reconstruction preserved the asymmetry ratio of mother to daughter vessels. When several options existed for segments with the closest diameter, the selection was made randomly using a uniform random number generator.

Histological Data

Once the tree was reconstructed down to 40 μm, the growth strategy changed from reconstruction of the tree bifurcation-by-bifurcation to subtree-by-subtree. Basically, a broken vessel whose diameter was in the range of 8–40 μm was allocated a subtree by finding a vessel in the input arteriolar file closest (smallest difference) to the cut vessel. The vessel closest to the desired diameter could be selected from anywhere along the measured subtree. The selected subtree was then pasted to the cut vessel. A check was made at each bifurcation to ensure that the mother-to-daughter diameter ratio was ≥ 1. The above process was repeated until the 'pasted' subtree had branches with diameters ≤ 8 μm. In cases where the diameters of the terminals were greater than 8 μm, the process of tree growth was repeated until the vessel diameter fell below 8 μm for each terminal segment. The stochastic search was similar to that outlined above and was continued until the reconstruction was terminated when the vessel reached a diameter ≤ 8 μm. The number of choices for the measured vessels that had diameters closest to that of the cut vessel were far greater for this part of the reconstruction than for vessels >40 μm. Again, when multiple choices existed, the selection was made randomly.

Mathematical Description of Branching Pattern

Once the entire arterial tree was reconstructed down to diameters ≥ 8 μm as outlined above, we assigned order numbers to the vessel branches by the Strahler system.[11] This method was first used by Horton,[4] a geologist, and later modified by Strahler.[21] In this method, the capillary blood vessels (defined as ≤ 8 μm) are referred to as Order 0. Two vessels of Order 0 meet to form a larger vessel of Order 1. When two arterioles of Order 1 meet, the confluent vessel was given an order number 2 and so on. But if a vessel of Order 2 merges with one of Order 1, the resulting vessel remains as Order 2; and so on. The Strahler ordering scheme was continued until every vessel segment in the tree was assigned an order number.

A diameter-defined criterion introduced by Kassab *et al.*[11] was then used to refine the order numbers with the objective to eliminate the overlap of diameter distributions that results from Strahler's model. Briefly, when two Order 1 vessels meet the confluent segment was assigned Order 2 if its diameter exceeded the diameters of the Order 1 vessels by an amount specified by a set of formulas or diameter criterion,[11] or remained as order number 1 if the diameter of the confluent was not larger than the amount specified by the formulas. When an Order 2 artery meets another Order 1 artery, the order number of the confluent was 3 if its diameter was larger by an amount specified by the diameter criterion, or remained at 2 if its diameter did not increase sufficiently. This process was continued until all arterial segments were arranged in increasing diameter and assigned the order numbers 1, 2, 3, . . ., n,. . ..

Once the entire coronary arterial tree was assigned order numbers, we defined those vessel segments of the same order connected in series as elements and determined the segments-per-element ratio (S/E). Furthermore, the connectivity of the various elements was presented in the form of a matrix, the component of which in row m and column n are the ratio of the total number of elements of order m sprung from elements of order n, divided by the total number of elements in order n. We called the results the connectivity matrix.[11] Finally, the longitudinal position matrix of the coronary arteries was also presented, the component of which in row m and column n is the fractional longitudinal

position of the vessels of order m which spring directly along the length of vessels of order n. We called the results the longitudinal position matrix.[13]

Stem-Crown Relationship

A vessel segment was defined as a stem and the entire tree distal to the stem was defined as a crown which is perfused by the stem.[23] The crown includes all vessels proximal to the stem including the capillary vessels (0 order vessels). Based on the minimum energy hypothesis and conservation of energy, we previously showed that certain structure-structure and structure-function relations exist.[26] For the structure-structure relationship, if A_s represents the mean cross-sectional area (CSA) of a stem and V and L represent the cumulative distal arterial volume and length of a crown, respectively, we derived the following equations:

$$\frac{V}{V_{\max}} = \left(\frac{L}{L_{\max}}\right)^{\alpha} \tag{1}$$

and

$$\frac{A_s}{A_{s,\max}} = \left(\frac{L}{L_{\max}}\right)^{\beta} \tag{2}$$

where $A_{s,\max}$, $V_{\max}$ and $L_{\max}$ correspond to the CSA of the most proximal stem to the arterial tree, the volume of the entire tree of interest, and the cumulative arterial length of the entire tree; α and β are constants that can be determined from a curve fit of the morphometric data. Equations (1) and (2) can be combined to yield a relation between the crown volume and stem CSA as

$$\frac{V}{V_{\max}} = \left(\frac{A_s}{A_{s,\max}}\right)^{\alpha/\beta} \tag{3}$$

We calculated the volume of the crown as the sum of the volume of all the individual vessel segments considered as circular cylinders as

$$V = \sum_{i=1}^{N} \frac{\pi D_i^2}{4} L_i \tag{4}$$

where D and L are the diameter and length, respectively, of each vessel segment i and N represents the total number of segments.

Data Analysis

All data presented in the Tables were averaged over each order number and compared to the previously published data on D, L, N, S/E, CM and LPM.[11,13] If X represents the mean D, L, N, S/E, CM or LPM, the percent difference ($\%X_\Delta$) between the previous (X_{previous}) and present values (X_{present}) can be determined as:

$$\%X_\Delta = \frac{X_{\text{previous}} - X_{\text{present}}}{X_{\text{previous}}} \times 100 \tag{5}$$

Obviously, data on $\%X_\Delta$ and the previously published mean values allow us to determine the mean values obtained using the present method.

RESULTS

The total number of vessel segments reconstructed for the RCA, LAD and LCx tree were 1.9, 2.04 and 1.15 million, respectively. These numbers only include vessel segments down to arterial capillaries.[10] All coronary arterial trees were found to have 11 orders from the proximal coronary artery to the first segment of capillary vessels. This result was the same before and after diameter-defined Strahler system.

The tree reconstruction was implemented over ten runs of the simulation. The run-to-run variation was fairly small as quantified by the coefficient of variance, CV (CV = SD/Mean) for each order number. We found the CV, for each order number, within a run to be significantly larger than those between runs. For example, the CV for Order 1 element diameter for the 10 runs (LCx arterial tree) was found to be 0.0098% as compared to 5.0% within a run. The CV over the ten runs was generally within 10% for diameters, and lengths and number of elements. Hence, all data summarized in the tables correspond to a single run with the exception of total number of vessels which were averaged over ten runs.

The $\%X_\Delta$ for the morphometric data for vessel elements of the RCA, LAD and LCx tree are shown in Table 2, respectively. The table shows the $\%X_\Delta$ of diameters, lengths, number of vessel elements and the segment-per-element ratio. The morphometric data on the diameters, lengths and number of vessels can be used to extract the mean branching characteristics of the tree. If n is the branching order and N_n and N_{n+1} are the total number of vessels of the branching order n and $n+1$, respectively, then the ratio $R_b = N_n/N_{n+1}$ is called the bifurcation ratio and is a function of n. If log N_n is plotted against n and a linear relationship is obtained, then the exponential of the negative of the slope of this line gives the bifurcation ratio R_b. In the coronary arterial tree R_b was not a constant. We evaluate the value of R_b at every order number n and summarize the mean $\pm$ SD as 3.14 ± 0.57, 3.13 ± 0.60 and 3.2 ± 1.14 for the RCA, LAD and LCx, respectively. Similarly, we computed the length ratio defined as $R_L = L_{n+1}/L_n$ and the diameter ratio as $R_D = D_{n+1}/D_n$. Our data show the diameter ratio for the RCA, LAD and LCx arterial trees as 1.79 ± 0.38, 1.75 ± 0.34 and 1.75 ± 0.33, respectively. Similarly, the length ratios were 2.24 ± 1.46 (RCA), 2.03 ± 0.92 (LAD) and 1.94 ± 0.42 (LCx).

The connectivity of one vessel element to another is given by the connectivity matrix, CM. The $\%X_\Delta$for the CM(m,n) are summarized in Table 3 for the RCA, LAD and LCx, respectively. The longitudinal position along a mother element at which a daughter element springs off

TABLE 2. The $\%X_\Delta$ as given by Equation (5) for diameters, lengths, number of elements (*N*) and segment-to-element ratio (S/E) of the RCA, LAD and LCx arterial trees.

Order	Diameter	Length	*N*	S/E
RCA elements				
1	5.7	8.0	25.3	1.1
2	10.9	3.6	−2.8	−4.3
3	7.4	2.8	0.0	9.1
4	13.3	19.8	1.2	3.0
5	28.8	19.6	11.0	−10.0
6	19.7	27.4	−23.0	−5.2
7	7.8	11.2	−18.9	3.1
8	4.7	7.2	−18.4	−0.4
9	−0.4	−8.2	0.0	−13.2
10	−7.8	19.3	−20.0	16.7
11	−0.1	−0.1	0.0	0.0
LAD elements				
1	2.0	10.4	18.7	17.4
2	4.9	−4.4	−3.8	−10.6
3	1.7	−25.5	−15.7	−16.0
4	9.5	32.0	2.2	−14.0
5	19.8	3.6	1.2	12.9
6	23.7	22.1	−45.1	−6.3
7	24.7	36.7	−34.8	20.6
8	13.0	11.4	−43.4	7.0
9	10.4	10.3	−37.8	8.3
10	27.7	43.8	−100.0	39.9
11	16.3	27.4	−100.0	−22.9
LCx elements				
1	2.0	10.4	−15.6	17.0
2	4.1	−10.3	−37.7	−16.8
3	−2.3	−40.3	−34.8	−23.0
4	−6.6	38.8	−8.6	−13.1
5	34.3	43.9	−65.1	27.3
6	40.1	36.1	−111.2	12.3
7	44.4	54.0	−200.0	18.9
8	34.2	36.8	−127.5	36.3
9	48.3	57.7	−390.0	34.1
10	58.0	59.5	−700.0	56.4

was characterized by the longitudinal position matrix, LPM. The $\%X_\Delta$ for the LPM (m,*n*) are summarized for the RCA, LAD and LCx tree in Table 4. The $\%X_\Delta$ for the CM(*n*,*n*) and LPM(*n*,*n*) are not computed because there are too few vessels for those components of the matrices.

Figure 3 shows the relationship between the normalized cumulative arterial volume of crown and the corresponding normalized cumulative length of crown for the RCA, LAD and LCx trees. Similarly, the relationship between normalized stem CSA and normalized cumulative length of crown is shown for the RCA, LAD and LCx trees in Fig. 4. Both relationships show a power law trend as described by Equations (1) and (2), respectively. The values of α and β were 1.43 and 0.93 (RCA); 1.41 and 0.92 (LAD); and 1.44 and 0.94 (LCx). The cumulative crown length of the RCA, LAD and LCx were 120 m, 116 m, and 66.5 m, respectively. The corresponding cumulative volumes were 1.3 ± 0.0012 ml (RCA), 0.97 ± 0.0009 ml (LAD) and 0.56 ± 0.0005 ml (LCx), respectively. The variation in volume from run to run was negligible as indicated by the small CV.

We computed the length of various pathways, from the proximal coronary artery to a particular capillary vessel, which equaled the number of Order 0 vessels in the reconstructed tree. Figure 5 shows the path length (sum of all segments along a particular path) distribution for RCA, LAD and LCx trees. The mean values ($\pm$1SD) for the distributions are 8.6 ± 3.6 cm (RCA), 5.8 ± 2.2 cm (LAD) and 6.3 ± 2.3 cm (LCx). The maximum path length for the RCA, LAD and LCx trees were found to be 14 ± 1.1 cm, 11 ± 1.4 cm and 11 ± 1.3 cm, respectively. The maximum path length corresponds to the length of the trunk down to the capillary vessel. The path lengths vary according to the route chosen which consists of different number of generations. Figure 6 shows the distribution of number of generations or level of branching for the RCA, LAD and LCx arterial trees with means ($\pm$1SD) of 52 ± 18, 44 ± 11 and 36 ± 10, respectively.

DISCUSSION

A Computer Reconstruction of Coronary Arterial Trees

We have developed a computer algorithm to reconstruct the branching pattern and vascular geometry of the entire coronary arterial tree, from the most proximal vessel segment to the inlet capillary vessels for the RCA, LAD and LCx trees based on partial cast and histological measurements. The majority of proximal vessels are exact since they were measured from the casts while the broken branches with the diameter distributions shown in Fig. 1 were reconstructed based on the measured data from the cast and histological sections. Once the connectivity (node-to-node connections) of the full tree was completely prescribed and the diameters and lengths of every segment noted, we used the diameter-defined Strahler system to assign order numbers to the entire tree.[11] The data on the diameters, lengths and number of vessels are tabulated for every order number. The data on the daughter-to-mother connectivity were also determined. It should be noted that the matrices provide statistical connectivity since they do not prescribe which exact daughter element arises from which mother element. Rather, they specify the fractional number of order *m* elements arising from order *n* elements. Finally, the fractional longitudinal positions of daughter vessels along the length of their mother vessel were computed.

With the exception of 3-D branching angles, the present model represents the architecture of the entire coronary arterial tree. Every path length from the proximal coronary artery to the capillary can be traced. The distribution of the various path lengths are shown in Fig. 5 for the RCA, LAD and LCx arterial trees. The shape of the distribution for the LAD and LCx arterial trees is normal while that of

TABLE 3. The $\%X_D$ as given by Equation (5) for the connectivity matrices of the RCA, LAD and LCx arterial trees.

	Order *m*										
Order *n*	1	2	3	4	5	6	7	8	9	10	11
RCA											
0	5	−77	−74	−45	—	—	—	—	—	—	—
1	—	31	29	57	−338	100	—	—	—	—	—
2		—	5	−17	67	40	86	—	—	—	—
3			—	0	29	82	82	68	100	—	—
4				—	−2	−72	37	10	50	—	—
5					—	1	12	11	−30	100	—
6						—	−11	−23	0	−11	−100
7							—	1	−25	21	0
8								—	−7	−25	0
9									—	−37	0
10										—	−17
LAD											
0	11	−69	−29	—	—	—	—	—	—	—	—
1	—	15	−12	61	—	—	—	—	—	—	—
2		—	5	50	−6	98	100	—	—	—	—
3			—	−16	−12	17	21	91	33	—	—
4				—	9	−68	21	15	38	50	—
5					—	5	34	6	10	75	—
6						—	10	−10	−27	22	—
7							—	4	−6	50	2500
8								—	9	33	0
9									—	25	44
10										—	−60
LCx											
0	11	−69	73	—	—	—	—	—	—	—	
1	—	10	−15	94	—	—	—	—	—	—	
2		—	−16	45	−13	—	—	—	—	—	
3			—	−8	−11	−80	64	—	—	—	
4				—	27	9	34	75	—	—	
5					—	10	39	64	36	—	
6						—	4	53	19	63	
7							—	−14	9	69	
8								—	51	56	
9									—	45	

RCA is bimodal. The bimodal distribution is reproducible from run-to-run and it arises because of the length of the trunk of the RCA. Unlike the LAD and LCx, the RCA has a longer trunk with a diameter that remains relatively uniform as it crowns the base of the heart. The large length of the trunk skews the path-length distribution to the right. We verified this hypothesis by computing the path-length for the RCA with the exclusion of the trunk and found the distribution to be nearly Gaussian similar to the LAD and LCx tree.

The total numbers of bifurcations or generations corresponding to the various path lengths are shown in Fig. 6 for the three arterial trees. It is apparent that the RCA tree has the maximum number of generations as compared to the LAD and LCx trees. The mean number of generations that span the arterial tree is also RCA > LAD > LCx tree. This is reasonable since the swine is right dominant and perfuses the largest myocardial territory similar to humans.

Comparison with Data Kassab et al., 1993

Kassab *et al.*[11] have previously developed a mathematical model of the coronary arterial tree based on the detailed morphometric data used in the present study. There are some key differences between the previous and present model. Previously, the data existed in hard records and the ordering scheme was carried out manually. In that approach, the assignment of orders was made iteratively since the coronary micro-vessels are cut at various diameters in the histological sections because of the three-dimensional branching pattern of the vessels. For vessels cut in the 8–9 μm diameter range, we distinguished between arterioles of Order 1 and capillaries of Order 0 as previously described.[11] Those vessels cut at larger diameters were then assigned order numbers statistically, in an iterative fashion as described by Kassab.[8] The process was initiated by assigning Orders 0 or 1 to the respective vessels and the

TABLE 4. The $\%X_D$ as given by Equation (5) for the longitudinal position matrices of the RCA, LAD and LCx arterial trees.

	Order *m*										
Order *n*	1	2	3	4	5	6	7	8	9	10	11
RCA											
0	−2	−2	−16	−44	—	—	—	—	—	—	—
1	—	−1	−2	−45	−30	100	—	—	—	—	—
2		—	−2	−8	−12	4	8	—	—	—	—
3			—	0	−4	−16	−14	−4	−28	—	—
4				—	7	−16	−5	−7	−7	—	—
5					—	2	−6	−1	−6	100	—
6						—	2	1	−7	−5	0
7							—	1	−4	−20	−1
8								—	−1	−19	−2
9									—	−4	12
10										—	−17
LAD											
0	−4	−5	−19	—	—	—	—	—	—	—	—
1	—	1	−6	−58	—	—	—	—	—	—	—
2		—	3	−14	13	−26	100	—	—	—	—
3			—	1	−12	−37	−6	−19	83	—	—
4				—	7	−17	−5	−26	12	2	—
5					—	3	−17	−2	−2	44	—
6						—	1	−6	−8	−18	—
7							—	−1	−4	−1	−84
8								—	−3	−3	−20
9									—	−17	0
10										—	13
LCX											
0	−4	−5	−16	—	—	—	—	—	—	—	
1	—	3	−3	23	—	—	—	—	—	—	
2		—	5	−15	57	—	—	—	—	—	
3			—	−5	−15	−22	−35	—	—	—	
4				—	2	−14	−9	−20	—	—	
5					—	8	−17	−24	−15	—	
6						—	−4	−18	−20	−31	
7							—	−2	−31	34	
8								—	−24	−30	
9									—	−9	

ordering was ascended along the tree according to Strahler's system. Of course, the tree could only be partially assigned order numbers because of possible cut branches that were larger than Order 1. First, we obtained some diameters of "derived" Orders 1 and 2 collectively for the several hundred arteriolar trees measured. We then used the resulting diameter distributions to define a diameter range according to the diameter-defined criterion for Order 1 and used this range to "assign" the order of cut vessels that fell in the range of Order 1. Hence, we obtained most of the data on diameters of Order 1 and further data on the diameters of Orders 2 and 3. We then used the diameter criterion of "derived" Order 2 vessels to assign the cut vessels in that diameter range. This process was continued until the orders of all cut segments of the trees were assigned order numbers. Finally, we required that the order number of any given cut segment to fall within the range of diameter criterion for each respective order.

Once the histological data were assigned order numbers, the next task was to mesh the histological data with those from polymer cast. Taking the mean and standard deviations of the vessels of Orders 3 and 4 in the histological sections, we assigned order numbers to the broken or terminal distal vessels in the tree casts, first according to the Strahler rules and then iterated according to the diameter-defined rule. The process outlined above was repeated until all the terminal segments were assigned order numbers and consquently all tree segments were ordered.

In the present study, the assignment of orders was done after the entire tree was reconstructed; first according to Strahler's scheme followed by the diameter-defined system. The mean diameters, lengths, number of vessels, S/E, connectivity and longitudinal position matrices reported here are within 10% of the previous data for the majority of orders as shown in Table 2. The largest differences for diameters (as large as 30%) occurred at Orders 5 and 6 for

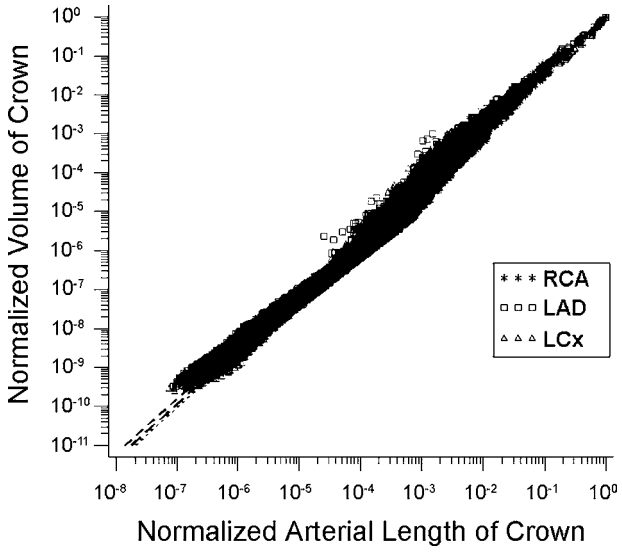

FIGURE 3. The relationship between the normalized arterial volume of crown and the corresponding normalized cumulative length of crown for (A) RCA, (B) LAD and (C) LCx arterial tree. The solid lines correspond to least square fits of the data according to the power law relation (Equation (1)) with a correlation coefficient of 0.999 for all three figures. The total number of data points shown are 957,821, 1,018,043 and 492,044 for the RCA, LAD and LCx arterial trees, respectively.

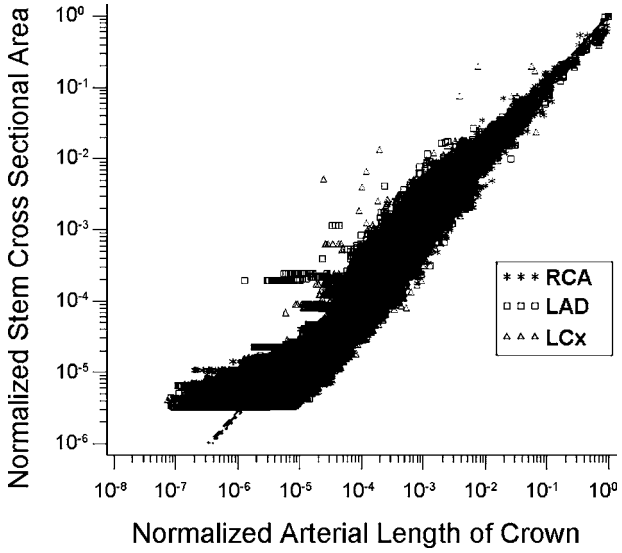

FIGURE 4. The relationship between normalized stem CSA and normalized cumulative length of crown is shown for the (A) RCA, (B) LAD and (C) LCx arterial trees. The solid lines correspond to least square fits of the data according to the power law relation (Equation (2)) with a correlation coefficient of 0.996, 0.997 and 0.997 for the RCA, LAD and LCx, respectively. The total number of data points shown are 957,821, 1,018,043 and 492,044 for the RCA, LAD and LCx arterial trees, respectively.

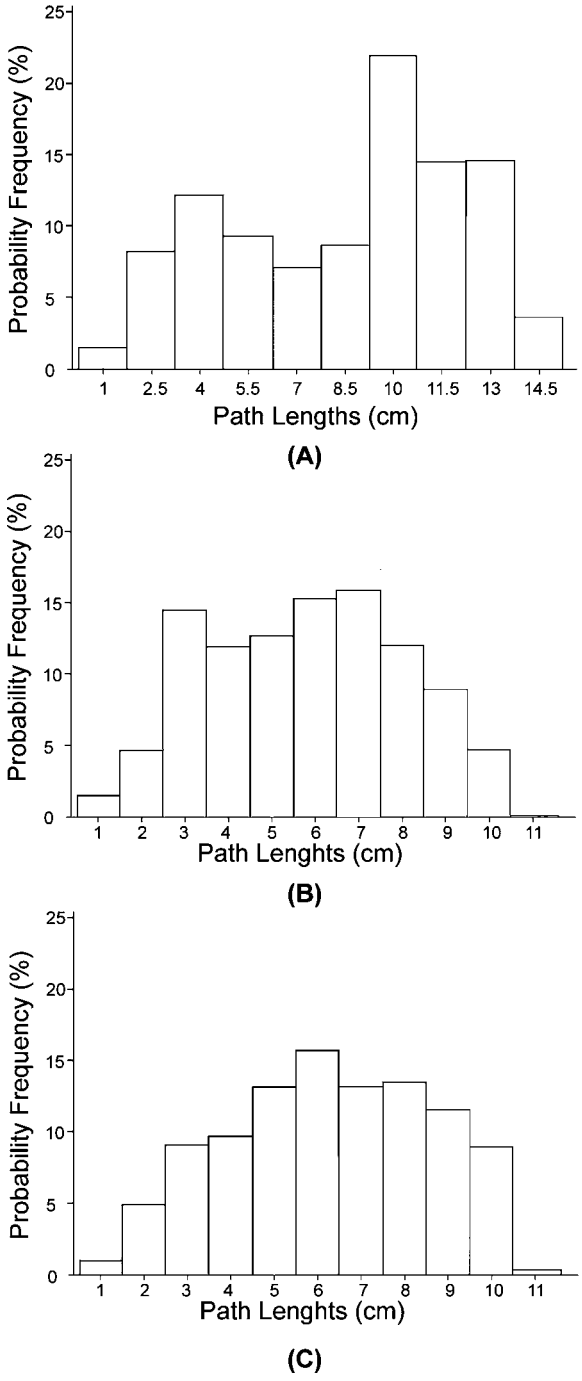

FIGURE 5. The distribution of path length for (A) RCA, (B) LAD and (C) LCx arterial trees. The total number of data points shown in Figures A, B and C are 853,876, 1,022,304 and 590,047, respectively.

the RCA and LAD arterial trees. Interestingly, the transition from histological to cast data occurs at Order 5. These differences led to a one-order increase in the total number of orders for the LCx arterial tree (i.e., 11 versus 10 previously). Consequently, the largest difference for the LCx

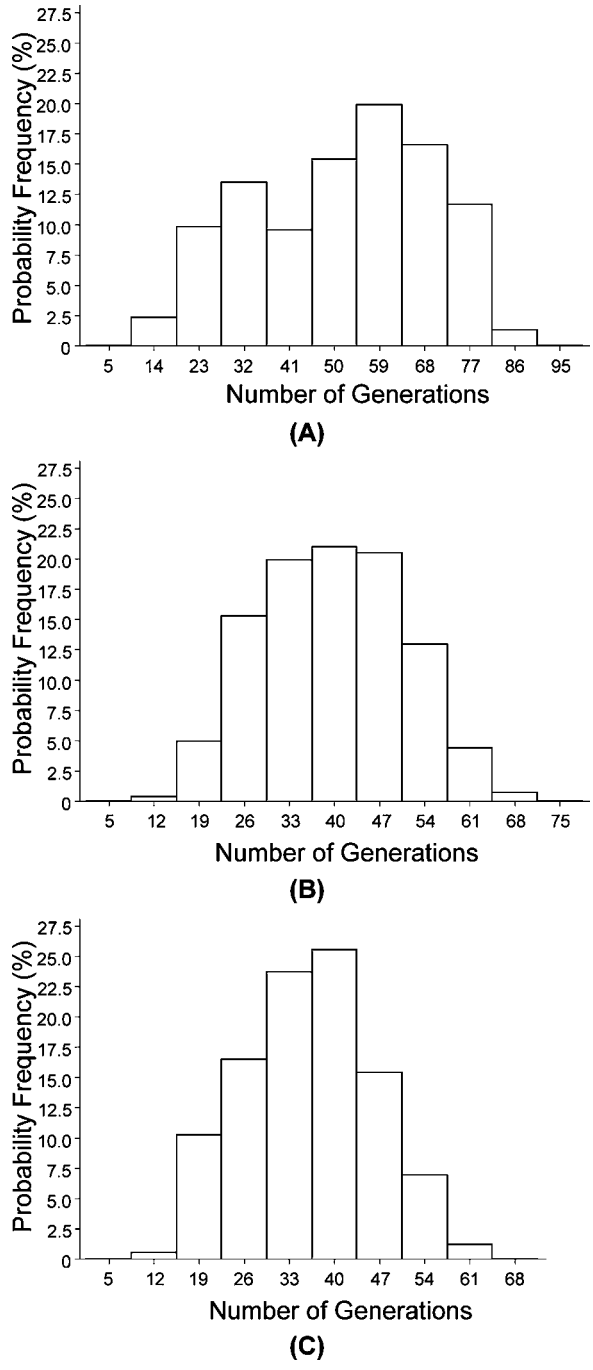

FIGURE 6. The distribution of the number of generations for (A) RCA, (B) LAD and (C) LCx arterial trees. The total number of data points shown in Figures A, B and C are 853,876, 1,022,304 and 590,047, respectively.

tree occurred at the highest order in the number of vessel elements. An even larger difference was observed for the number of vessels for highest orders of the LAD tree. This occurred because the total number of elements of LAD arterial tree was found to be 2 (in 6 out of 10 simulations) as compared to a single element as previously reported. In those 4 simulations where we found a single element of Order 11, the S/E exactly matched the previously reported value.

Despite the differences in the number of vessels at each order, the total number of vessels for the entire coronary arterial tree for the RCA, LAD and LCx system were very similar for the two models: 15.7%, 9.7% and −23.0%, respectively. Similarly, the diameter, length and number ratios were very similar for the two models. The differences in the R_D, R_L and R_b were 1.1%, −5.7%, 10.3% (RCA); 4.9%, 0.5%, 10.8% (LAD) and 7.4%, 11.7%, 10.4% (LCx tree). As expected, the $\%X_\Delta$ are largest for the LCx arterial tree because of the difference in the total number of orders.

Tables 3 and 4 provide a comparison of the present and previous models for the CM and LPM. It is apparent that most of the diagonal elements of both matrices (CM(n, $n+1$) and LPM (n, $n+1$)) are similar for the two models (i.e., small $\%X_\Delta$). The LPM values are more similar between the two models than the CM because of the constrained values of LPM between 0 and 1. The off diagonal components of CM and LPM matrices vary more between the two models than the diagonal terms. This may be due to the differences in the number of data points which is greatest for the diagonal components of the matrices.

Comparison with Other Tree Growth Algorithms

A number of studies have focused on the growth simulation of coronary arterial system. VanBavel and Spaan[22] have previously reconstructed coronary vascular trees for vessel branches smaller than 0.5 mm in diameter. Their approach was based on the determination of the relation between the diameter of mother and larger daughter; mother and smaller daughter vessel; and the diameter-length relationship. They modeled the stochastic features of the tree based on the scatter of the measured data. Coronary arterial tree models have also been constructed based on the fractal principal,[18] constrained constructive optimization,[7] and Monte Carlo method.[25]

Recently, Beard and Bassingthwaighte[1,2] have developed an avoidance algorithm which is based on the morphometric measurements of Kassab *et al.*[11] They reconstructed the vascular branching pattern in a cylindrical model of the heart. Smith *et al.*[20] also using Kassab's morphometric data,[11] have developed a similar algorithm to map the distribution of vascular elements in the myocardium as a nonlinear optimization of individual branch angles based on the minimum shear stress hypothesis and whole organ vessel distribution. Using this algorithm, a finite element model of the largest six generations of arterial coronary tree has been generated. The vascular network was geometrically embedded in the finite element ventricular model of Nielson.[16] Although the model in the present study lacks a spatial geometry, the focus is on the reconstruction of full connectivity and segment geometry. The goal of future

studies will be to map the circuit model, along with the branching angle data, onto a realistic 3-D geometry of the heart.

Optimization Rules of the Coronary Arterial Tree

The generalization of Murray's law[15] to a stem-crown system led to the power law relations expressed by Equations (1) and (2). Zhou *et al*.[26] previously validated those relations for exact partial data (vessels proximal to 0.5 mm) and for a full idealized symmetric model.[14] Our present results show that the design rules are also valid for the full asymmetric models (Figs. 3 and 4). The range of power law exponents are remarkably uniform ($\alpha = 1.41 - 1.43$; $\beta = 0.92 - 0.94$) for all three arterial trees. The exponent of Equation (3) was similarly uniform ($\alpha/\beta = 1.53 - 1.54$). Equation (3) is an important structure-structure relation in that it allows the prediction of the crown cumulative volume for a given stem CSA.

Some Validation of Tree Model

The cumulative volume of blood in each arterial tree calculated from the present model is 1.3 ml (RCA), 0.97 ml (LAD) and 0.56 ml (LCx). These data are similar to our experimental measurements of the volumes of the cast which yielded 1.4 ml, 0.98 ml and 0.57 ml for the RCA, LAD and LCx, respectively.[11] The total length of the tree trunk was also compared to experimental data. The model predicts length of 14.5 cm (RCA), 10.8 cm (LAD) and 10.8 cm (LCx). Since the length of each vessel segment is related to the diameter of the vessel as a power law, the majority of the length belongs to the trunk of the epicardial tree. Our experimental cast measurements of the epicardial RCA, LAD and LCx lengths were 13.6 cm, 10.1 cm and 9.2 cm, respectively.

Critique of Model

The present reconstruction assumes that the larger daughter vessel is smaller than or equal to the mother vessel; i.e., the tree tapers from proximal to distal. This assumption is, of course, consistent with the majority of measured data. In approximately 10% of the data, however, we do find deviations from this rule; i.e., daughter may be slightly larger than mother vessel. It is unclear whether those measurements are artifacts of casting technique or represent local vasoconstriction of some vessels. In any case, those features were not represented in the present simulation. An additional approximation should be noted. When assigning daughter vessels to a terminal vessel, both the diameter and the length must be assigned to each daughter. The lengths of the reconstructed segment were obtained by selecting the lengths corresponding to the vessels of the bifurcation. In some cases, however, this information was missing because the vessel was broken and a search was made in the input data for a vessel with a diameter closest (smallest difference) to the generated daughter diameter for which the length information was available.

The reconstruction of cast data was made one-bifurcation at a time while that of histological data was made one-subtree at a time. The difference in growth algorithms was necessitated by the observation that an unrealistically long string of arteriole vessels (S/E ratio in excess of 10) resulted when growth was attempted one-bifurcation at a time. This underscores the importance of knowing the correlation of the vessels beyond the mother-daughter unit; i.e., mother-daughter-granddaughter, etc. This effect was more profound in the microvasculature because of the smaller asymmetry of micro-vessels; i.e., the change in diameter of vessels is smaller at each bifurcation.[6,9]

Although the assignment of tree orders was automated, the order of the trunk was checked manually. This was necessitated by the observation that 2 out of 10 simulation runs for the RCA and LAD trees yielded 12 orders. An inspection of these trees revealed that the change in order 11–12 occurred very proximal in the tree (2 or 3 segments from the root). These trees acquired an extra order during Strahler's ordering scheme. Due to the nature of the diameter-defined scheme, the highest order cannot be eliminated automatically. The upper range of the diameter-defined criterion is obtained from the higher order. For the highest order, however, the upper bound cannot be defined and the decision has to be made upon inspection taking into account the diameter ratio at a bifurcation. This minor labor is well justified since the number of large trunk vessels is small. Strictly speaking, the largest trunk of the tree deviates from a tree structure and should be handled as a special case.

Significance of Model

The present model will impact two important areas of vascular research: (1) automation of vascular reconstruction and (2) establishment of an anatomical foundation for blood flow analysis. Recently, there has been strong effort to automate the process of vascular reconstruction using computerized tomographic (CT) imaging technology.[3] Ritman and colleagues have successfully used 3D micro-CT imaging to provide the 3D geometry of the coronary arterial tree of the rat heart.[5] Bassingthwaighte and colleagues are also in the midst of developing automation technology for the vascular reconstruction of rabbit heart (personal communication). Their approach consists of 3-D reconstruction of the coronary arterial tree from frozen sections of the myocardium whose vasculature is filled with fluorescent polymer. Hence, the next important step is to develop an automated algorithm to extract detailed morphometric data on the diameters, lengths, number of vessels, connectivity and branching angles from the reconstructed trees.[24] In the process, it is imperative to develop a computer algorithm

to generate a full vascular tree from a partial image since it is impossible to image or count every single vessel in a coronary vascular network. The present study offers such a scheme.

On the second issue, a detailed circuit with anatomical data on the branching pattern and geometry of the vasculature is required in order to carry out a complete analysis of blood flow in a vascular network. Advancements in high performance computers make it possible now to attempt anatomically-based computational models rather than the "lumped" models used in the past where the anatomical details of the coronary vascular system are ignored.[19] This is a philosophy to minimize the number of ad hoc assumptions in the formulation of coronary blood flow analysis. This is an attempt to move away from the "black box" approach and to understand the coronary circulation in greater depth.

ACKNOWLEDGMENTS

This research was supported in part by the National Institute of Health-National Heart, Lung, and Blood Institute Grant 2 R01 HL055554-06 (GSK), R01 HL67159-03 (SM) and American Heart Association 0315029Y (GSK). Dr. Kassab is an American Heart Association (AHA) Established Investigator and Mr. Mittal is an AHA Pre-Doctoral Fellow.

REFERENCES

[1]Bassingthwaighte, J. B., D. A. Beard, Z. Li, and T. Yipintsoi. Is the fractal nature of intraorgan spatial flow distributions based on vascular network growth or on local metabolic needs? Vascular Morphogenesis: In Vivo, In Vitro, In Mente, edited by C.D. Little, V. Mironov, E.H. Sage, Boston: Birkhauser, 1998.

[2]Beard D. A., and J. B. Bassingthwaighte. The fractal nature of myocardial blood flow emerges from a whole-organ model of arterial network. *J. Vasc. Res.* 37:282–296, 2000.

[3]Beighley, P. E., P. J. Thomas, S. M. Jorgensen, and E. L. Ritman. 3D architecture of myocardial microcirculation in intact rat heart: A study with micro-CT. *Adv. Exp. Med. Bio.* 430:165–175, 1997.

[4]Horton, R. E. Erosional development of streams and their drainage basins; hydrophysical approach to quantitative morphology. *Bull. Geol. Soc. Am.* 56:275–370, 1945.

[5]Jorgensen, S. M., O. Demirkaya, and E. L. Ritman. Three-dimensional imaging of vasculature and parenchyma in intact rodent organs with X-ray micro-CT. *Am. J. Physiol.* 275 (*Heart Circ. Physiol.* 44):H1103–H1114, 1998.

[6]Kalsho, G., and G. S. Kassab. Bifurcation asymmetry of the porcine coronary vasculature and its implications on coronary flow heterogeneity. *Am. J. Physiol Heart Circ Physiol* 287:H2493–H2500, 2004.

[7]Karch, R., F. Neumann, M. Neumann, and W. Schreiner. Staged growth of optimized arterial model trees. *Ann. Biomed. Eng.* 28:495–511, 2000.

[8]Kassab, G. S. Morphometry of the Coronary Vasculature in the Pig. Ph.D. Dissertation, San Diego: University of California, 1990.

[9]Kassab, G. S., A. Schatz, K. Imoto, and Y.C. Fung. Remodeling of the bifurcation asymmetry of right ventricular branches in hypertrophy. *Ann. Biomed. Eng.* 28:424–430, 2000.

[10]Kassab, G. S., and Y. C. Fung. Topology and dimensions of the pig coronary capillary network. *Am. J. Physiol.* (*Heart Circ. Physiol.* 36):H319–H325, 1994.

[11]Kassab, G. S., C. A. Rider, N. J. Tang, and Y. C. Fung. Morphometry of pig coronary arterial trees. *Am. J. Physiol.* 265 (*Heart Circ. Physiol.* 34):H350–H365, 1993.

[12]Kassab, G. S., D. Lin, and Y. C. Fung. Morphometry of the pig coronary venous system. *Am. J. Physiol.* 267 (*Heart Circ. Physiol.* 36):H2100–H2113, 1994.

[13]Kassab, G. S., E. Pallencaoe, A. Schatz, and Y. C. Fung. The longitudinal position matrix of the pig coronary vasculature and its hemodynamic implications. *Am. J. Physiol.* (*Heart Circ. Physiol.* 42):H2832–H2842, 1997.

[14]Kassab, G. S., J. Berkley and Y. C. Fung. Analysis of pig's coronary arterial blood flow with detailed anatomical data. *Ann. Biomed. Eng.* 25:204–217, 1997.

[15]Murray, C. D. The physiological principle of minimum work. I. The vascular system and the cost of blood volume. *Proc. Natn. Acad. Sci., USA*, 12:207–214, 1926.

[16]Nielsen, P. M. F., I. J. Le Grice, B. H. Smaill, and P. J. Hunter. Mathematical model of geometry and fibrous structure of the heart. *Am. J. Physiol.* 260, *Heart Circ. Physiol.* 29:H1365–H137, 1991.

[17]Poole, D. L., and A. K. Mackworth. CIspace: Tools for Learning Computational Intelligence. In: *Proceedings of the Workshop on Effective Interactive AI Resources*, Seattle, WA, American Association for Artificial Intelligence, August 2001, p. 5.

[18]Qian, H., and J. B. Bassingthwaighte. A class of flow bifurcation models with lognormal distribution and fractal dispersion. *J Theor Biol.* 205(2):261–268, 2000.

[19]Smith, N. P., and G. S. Kassab. Analysis of coronary blood flow interaction with myocardial mechanics based on anatomical models. *Phil. Trans. R. Soc. Lond. A* 359:1251–1263, 2001.

[20]Smith, N. P., A. I. Pullan, and P. I. Hunter. The generation of an anatomically accurate geometric coronary model. *Ann. Biomed. Eng.* 28(I):14–25, 2000.

[21]Strahler, A. N. Hyposometric (are altitude) analysis of erosional topology. *Bull. Geol. Soc. Amer.* 63:1117–1142, 1952.

[22]VanBavel, F., and J. A. E. Spaan. Branching patterns in the porcine coronary arterial tree. Estimation of flow heterogeneity. *Circ. Res.* 71:1200–1212, 1992.

[23]Wahle, A., E. Wellnhofer, I. Mugaragu, H. U. Sauer, H. Oswald, and E. Fleck. Quantitative volume analysis of coronary vessel systems by 3-D reconstruction from biplane angiograms, *IEEE Medical Imaging Conference 1993*, San Francisco, IEEE Press, 1993/4, 2, 1217–1221.

[24]Wan, S.-Y., E. L. Ritman, and W. E. Higgins. Multi-generational analysis and visualization of the vascular tree in 3D micro-CT images. *Comput. Biol. Med.* 32:55–71, 2002.

[25]Wang, C. Y., I. B. Bassingthwaighte, and L. J. Weissman. Bifurcating distributive system using Monte Carlo method. *Math. Comput. Model.* 16(3):91–98, 1992.

[26]Zhou, Y., G. S. Kassab, and S. Molloi. On the design of the coronary arterial tree: A generalization of Murray's law. *Phys. Med. Bio.* 44:2929–2945, 1999.